Electromicrogravimetric study of underpotential deposition of Co on textured gold electrode in ammonia medium

Antonio Montes-Rojas,* Luz María Torres-Rodríguez and Cesar Nieto-Delgado

Received (in Montpellier, France) 3rd April 2007, Accepted 8th June 2007
First published as an Advance Article on the web 27th June 2007
DOI: 10.1039/b704891b

Formation of a layer of a metal M on a foreign metal substrate, S, at potentials positive to its reversible potential, E_r, (underpotential deposition, UPD) is a phenomenon that appears only in some systems. In the case of the UPD process of Co on a gold substrate, there is still a controversy about its existence, for which reason, in this study, voltammetry and chronoamperometry were coupled with a quartz microbalance in ammonium solution to better understand its formation mechanism. The results obtained show that the Co forms only one layer on the substrate before the bulk deposition of cobalt occurs. During the UPD process, the Co atom completely transfers its two electrons to the electrode and is adsorbed as a discharged species. The monolayer charge density, determined by electromicrogravimetry, is 448 μC cm^{-2} and probably corresponds to a commensurate overlayer on the gold substrate. In addition, the UPD process is controlled by adsorption as shown by voltammetric experiments. Finally, the analysis of the process of Co monolayer destruction (desorption) shows a mechanism different from that in the formation process, possibly due to H adsorption on the substrate produced during the process of adsorption of Co.

1 Introduction

The underpotential deposition (UPD) is defined as the process of deposition of one metal (M) onto a dissimilar metal substrate (S) at a positive Nernst potential for bulk deposition, and it is undoubtedly one of the most extensively studied processes in surface electrochemistry. A metal UPD process involves not only a unique possibility to study the first step of the electrocrystallization of a metal on a foreign substrate, but also allows variation of its coverage as a function of the potential to be used in electrocatalysis.

UPD studies have been carried out with polycrystalline metal electrodes,[1,2] well-defined single crystal surfaces[3,4] or, more recently, with highly ordered electrodes.[5,6] Numerous bimetallic systems were investigated, mainly because of their unique structural, electronic, magnetic and chemisorption properties compared with either of the bulk metal components.

In recent years, Co monolayers on Au or Ag have received attention from several authors and this system has been studied by different techniques[7–17] because of the giant magnetoresistance properties of Co. Therefore, this metal is certain to be placed at the center of many studies in the coming years.

An exciting issue concerning this metal is its UPD process onto gold substrates which has been considered from two viewpoints. In the first, Mendoza-Huizar *et al.*[18–20] reported a series of studies relating to cobalt UPD onto different substrates. These authors found that a cobalt adlayer is formed on a polycrystalline gold electrode during application of potential in the UPD region. In addition, formation of this cobalt adlayer involves the simultaneous presence of both adsorption and 2D nucleation mass transfer-controlled processes. More recently, Flis-Kabulska[21] studied Co electrodeposited on Au(111) from $CoSO_4$ solutions in 0.5 mM H_2SO_4. Using STM and cyclic voltammetry he showed that the electrodeposition started at underpotential and that the substrate was covered by about one monolayer. In the second viewpoint, Schindler *et al.*[22] have mentioned that in the Au/Co^{2+} system there is a relatively weak substrate–deposit interaction compared to the strong interaction characteristic of underpotential deposition systems. In this same viewpoint, Kleinert *et al.*[23] investigated the initial stages of Co deposition onto Au(111) and Au(100) electrodes in neutral sulfate solutions and they reported that the UPD process could be excluded. These authors reported that Co formed monoatomic high islands only at the very beginning of growth. Further deposition on top of these islands starts rather quickly, leading to a twin layer which soon covers the whole surface. Finally, after completion of the twin layer, the third layer starts growing.

These results are interesting since it is known that the UPD process of a metal onto a substrate occurs when the work function of the latter is larger than that of the deposited metal. In this case this rule is observed since the value of the work function of the substrate is superior to that of the cobalt[24] (4.78 and 4.70 eV, respectively).

Despite these results, the question of whether or not the initial stage of electrochemical deposition of Co on Au proceeds at underpotentials remains open and in this sense, we propose to use a special tool that could clarify this issue.

Laboratorio de Electroquímica, Centro de Investigación y Estudios de Posgrado, Facultad de Ciencias Químicas, Universidad Autónoma de San Luis Potosí, Av. Dr Manuel Nava No. 6, Zona Universitaria, SLP, SLP México 78210. E-mail: antonio.montes@uaslp.mx; Fax: (0052) 48262371; Tel: (0052) 48262372

Many techniques can be used to obtain information on this kind of system, nevertheless, the electrochemical quartz-crystal microbalance (EQCM) has made a significant impact in recent years as an *in situ* technique, capable of measuring the mass increase or decrease at the electrode surface as a function of potential[25–27] using the Sauerbrey expression:

$$\Delta m = -C_f \Delta f \quad (1)$$

where C_f, the sensitivity constant,

$$C_f^{-1} = \frac{2f_o^2}{(\rho_q \mu_q)^{1/2}}$$

depends only on the properties of the quartz resonator itself: μ_q and ρ_q are the shear modulus and density of quartz, respectively, and f_o is the fundamental frequency of the resonator.

This equation holds only under certain conditions such as that the resonant frequency shifts by no more than 2% of the fundamental.

These properties of EQCM permitted the UPD systems to become popular targets of EQCM study with a wide variety of substrates, metals and electrolytes.

In this paper we report new results obtained on this system when the Co UPD process is examined by cyclic voltammetry and chronoamperometry coupled with a quartz-crystal microbalance.

2 Experimental

The test solution was prepared from $Co(NO_3)_2$ (Baker) in 10^{-3} M $(NH_4)_2SO_4$ (Sigma) 1 M concentration, and ultrapure water. The pH of the solutions was fixed with NaOH (Sigma) at 9.3 to diminish interferences of hydrogen evolution and to have the predominant species $[Co(NH_3)_6]^{2+}$. Prior to each experiment the solution was degassed by bubbling N_2 through the solution for at least 10 min, during which the atmosphere was saturated with this gas.

The electromicrogravimetric measurements were performed with a PAR model 273A coupled with a quartz microbalance Seiko model QCA922.

EQCM experiments were performed with polished AT-cut gold-coated 9 MHz quartz crystals (Seiko) of mass sensitive area (S_{geo}) 0.196 cm^2. Before each experiment, all the electrodes were subjected to a cyclic voltammetric treatment in 0.5 M H_2SO_4. Next, the electrodes were transferred to the test solution. This procedure gives rise to reproducible and well-defined voltammetric responses, which bear witness to the quality of the electrodes and the cleanliness of the working solutions.

The sensitivity factor in the Sauerbrey equation (eqn (1)) was determined by chronoamperometric silver deposition and its value was very close to the theoretical value ($1.714 \pm 0.012 \times 10^8$ Hz g^{-1} cm^2). The electroactive area (S_{elect}) of these working electrodes was determined using the adsorption–desorption process of oxygen onto gold.[28] Using S_{geo} and S_{elect} the roughness factor was calculated, defined by $r = S_{elect}/S_{geo}$ which was 1.25 ± 0.04.

Potentials were measured against and are quoted *versus* the Ag|AgCl|3 M NaCl reference electrode and a platinum wire was used as counter-electrode. All the experiments were performed at room temperature.

3 Results and discussion

3.1 Substrate characterization

Fig. 1 shows a typical current–potential (*I–E*) curve obtained at a Au film electrode supported on quartz in 0.5 M H_2SO_4 after the cyclic voltammetric procedure. This voltammogram possesses certain characteristics such as the very small current observed in the zone A which corresponds to charging of the electrical double layer and this characteristic is a criterion for the cleanliness of the surface of our electrodes. In addition, the current peaks that appear in the zone B are associated with the processes of oxide formation and reduction on gold in the presence of specific adsorption.[29]

According to Hamelin *et al.*[30] and Štrbac *et al.*,[31] the position of anodic peaks on the potential axis and their shape are typical of each crystalline orientation, for example the most important anodic current peak in the region B at +1442 mV is characteristic of the oxidation of terraces of the (111) orientation (less active sites). However, this peak does not have such an important intensity as that of a true mono-crystal, perhaps because our electrodes are made up of small grains that produce a very rugged surface and consequently a decrease in its intensity. In addition, the small prepeaks probably correspond to the formation of an OH monolayer on defects (more active sites) or on other plane crystallines.[32]

Furthermore, cyclic voltammetry carried out in a 5 mM $CuSO_4$ + 0.5 M H_2SO_4 solution revealed the two-stage formation of a Cu UPD layer typical of a well-defined Au {111} substrate[33,34] and not only one current peak distinctive of a polycrystalline substrate.[35,36] Also, the change of frequency–potential response [Fig. 2] showed a behavior similar to that reported by Borges *et al.* and Watanabe *et al.*, who used textured gold substrates.[37,38]

Finally, our X-ray pattern of the thin gold layer showed a big peak at 38.37 (2θ), which is associated with the plane mentioned above {111}. So, all these results show that our electrodes have a textured surface in the direction {111}.

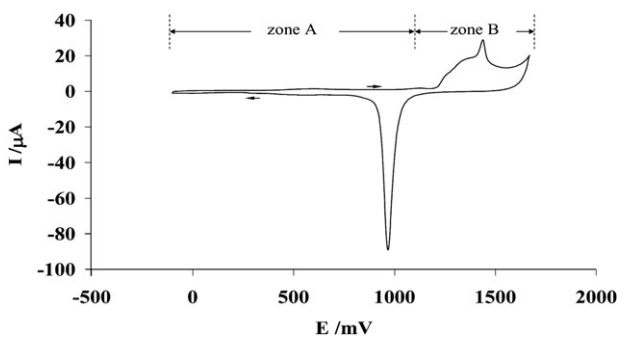

Fig. 1 Current–potential (*I–E*) curve for Au EQCM film obtained in 0.5 M H_2SO_4: scan rate, 50 mV s^{-1}. The geometric surface (S_{geo}) is 0.1965 cm^2.

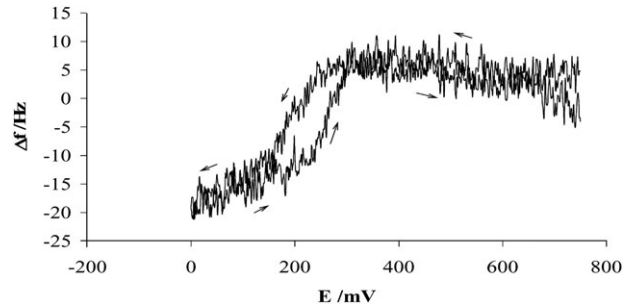

Fig. 2 Change of frequency (Δf) as a function of potential of a Au EQCM electrode in 5 mM $CuSO_4$ + 0.5 M H_2SO_4 solution. The scan rate was 5 mV s^{-1}.

3.2 Voltammetric characterization of Co UPD on Au

A large potential zone was scanned using the electrodes of EQCM in $(NH_4)_2SO_4$ 1 M solution adjusted to pH 9.3 in the absence of metallic ion with the aim of establishing the effect of the support electrolyte on the voltammogram and the variation of frequency *vs*. potential curve, Δf–E. These curves are shown in Fig. 3.

Between +350 mV and −650 mV, the curve j–E shows a small constant current of about ±0.56 μA cm^{-2} relative to the electrical double layer charge. At potentials more negative than −650 mV, the reduction of H^+ to H_2 starts to take place at the substrate. This process has been associated with an increase in the cathodic current in the voltammogram.

In the case of the variation of frequency *versus* potential curve, (—) Δf–E, in the beginning of the direct potential scan at 0 mV, the frequency variation value is only of ±2 Hz up to −700 mV. This small change of frequency value implies that there are no processes with a mass change produced in this potential region. At potentials more negative than −700 mV the Δf decreases up to −17 ± 2 Hz. It is important to mention that this value is not really associated with an increase of the mass on the substrate but possibly with a change of viscosity on the substrate resulting from the process of reduction of H^+ to H_2 which begins at about −780 mV. As the potential scan is reversed the behavior of the Δf becomes almost constant at −8 ± 2 Hz. Only when the potential scan is about to end is the value of Δf the same as in the beginning.

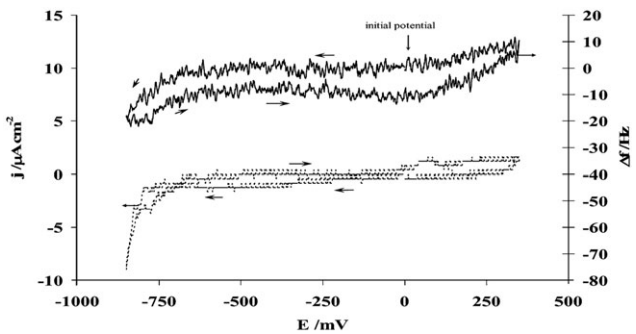

Fig. 3 Voltammogram, j–E, (—) and variation of frequency *versus* potential curve, Δf–E, (—) of the gold electrode obtained in the supporting electrolyte $(NH_4)_2SO_4$ 1 M pH 9.3. The scan rate was 5 mV s^{-1}.

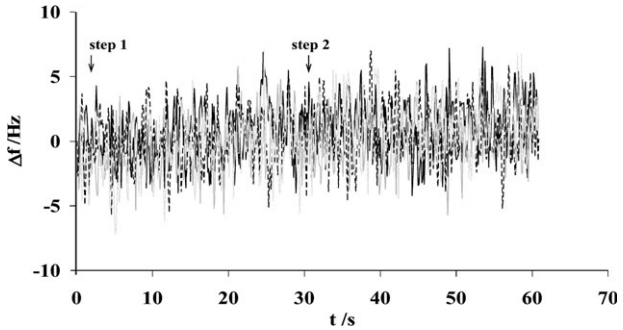

Fig. 4 Some experimental Δf–t curves recorded in the UPD zone of Au in 1 M $(NH_4)_2SO_4$ (pH 9.3) solution by means of a program of three potential steps. In all cases the starting potential and the final potential (step 2) were +250 mV. The second potential step (step 1) was (a) 0 mV, (b) −200 mV, (c) −400 mV, (d) −450 mV and (e) −500 mV.

At this point of the study, it was proper to wonder if these responses had a contribution from adsorption of NH_3 molecules on the electrode. To clear up this doubt, potential pulses were applied in this region and the Δf response was recorded (Fig. 4).

Fig. 4 shows only some of the curves obtained in these experiments. As may be observed, the common feature of the curves is that they all have the same behavior, *i.e*., frequency variation is practically constant during the pulse time and independent of the applied potential. The Δf value recorded was ±3 Hz during all experiments, which represents a minimum variation of Δf, equivalent to that obtained in the potential scan toward negative potentials from Fig. 3.

These results confirm that frequency variation as a consequence of the process of adsorption of NH_3 species on the electrode is not important in the UPD region.

The next step was to define the UPD region of the Co/Au system, for which reason it was necessary to obtain the I–E curve in the presence of metallic ion in solution. Fig. 5 shows a typical I–E curve obtained at a Au electrode in the presence of Co(II) 10^{-3} M.

The potential region was scanned between +100 mV and −1100 mV. The experiment started at +100 mV up to −1100 mV and then it was reversed to the starting potential. During the direct potential scan, only one current peak appeared at −480 mV associated with the Co UPD process

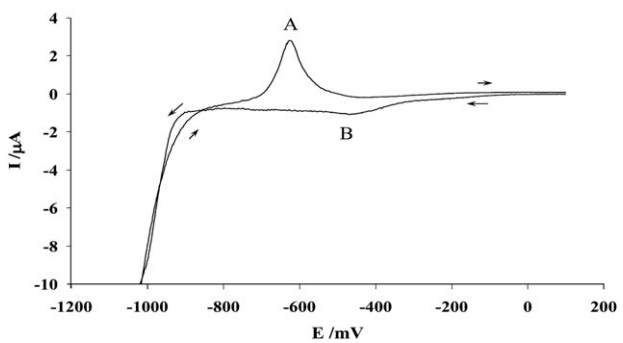

Fig. 5 Voltammogram at 5 mV s^{-1} for Au EQCM electrodes in $(NH_4)_2SO_4$ 1 M (pH 9.3) + 1 mM Co(II).

(peak B). It is important to mention that this voltammetric response is very similar to that reported by Huizar *et al*. in the same Co/Au system using a monocrystalline substrate Au(111),[18–20] which confirms the ordered surface of our electrodes. In addition, an important characteristic of this response is that the unique current peak associated with the UPD process of cobalt reveals that the overlayer formation–destruction processes have a different nature from, for example, the Tl UPD system which exhibits two complementary peaks for adsorption–desorption processes in the UPD region.[39] As the electrode potential changes to more negative values, the current increases rapidly due to the bulk cobalt deposit on the Au electrode and simultaneously due to the hydrogen evolution reaction. On the other hand, during the inverse potential scan, two crossovers of the cathodic and anodic branches at −962 mV and −754 mV can be seen. The more cathodic crossover (−962 mV) is associated with the nucleation process of a new phase[40] and the parameters of the nucleation-growth mechanism can be taken. At potentials more negative than −962 mV, lower current is found during the scan toward positive potentials than toward negative potentials, probably due to the changes in the interface concentration of $[Co(NH_3)_6]^{2+}$ ions, as a result of the deposition process.[40,41] However, in the range between −962 mV and −754 mV, the current shows an opposite behavior in both scan directions because the energy required for cobalt deposition on the cobalt film, during the forward sweep, is lower than that required for cobalt deposition on the Au electrode modified by the UPD Co.

As the electrode potential was changed toward more positive values, only one peak of anodic current at −620 mV was observed (peak A). This peak is related to the oxidation of cobalt deposited previously during the direct potential scan.

In order to ensure that the cathodic peak at −480 mV (peak B) actually occurs due to the UPD process of Co onto Au, a previous analysis of this peak as a function of scan rate was carried out. We obtained *I*–*E* curves at different scan rates and we prepared curves of current peak as a function of scan rate as shown in Fig. 6.

In this figure, a linear relationship between the cathodic peak current density (*j*) and the scan rate (*v*) associated with the peak B can be observed. This tendency implies that the Co atoms are adsorbed on different types of sites present at the substrate, as has been pointed out by different authors.[42–45] In this case, it shows that the UPD process is controlled by

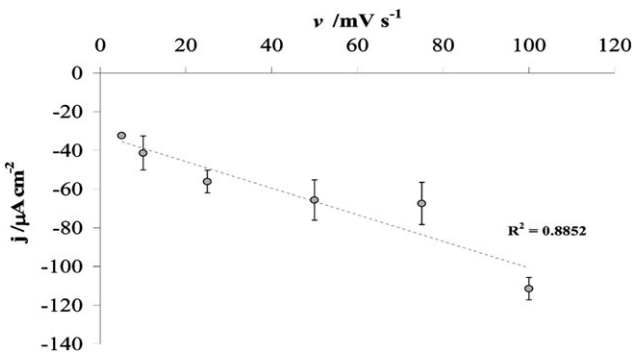

Fig. 6 Plot of the experimental cathodic peak current density (*j*) as a function of scan rate (*v*) for peak B (see Fig. 5).

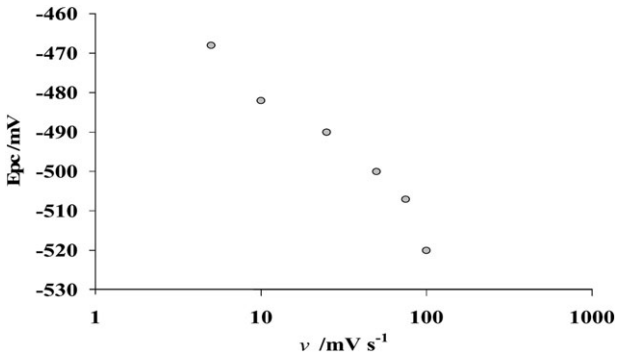

Fig. 7 Plots of the experimental cathodic peak potential as a function of scan rate (*v*) for peak B (see Fig. 5).

adsorption and confirms that the peak B corresponds to a Co UPD process on the gold electrode.

In addition, Fig. 7 shows the behavior of the cathodic peak potential, *E*pc, as a function of the sweep rate in the range of 5–100 mV s^{-1}. We can see that the peak shifts in the negative direction with an increasing sweep rate, as a result of the irreversible behavior of the system.[42,46]

In relation to this discussion it is important to say that Kleinert *et al*.[23] have reported a clear pre-wave for the Co deposition on Au(100) around −0.8 V *versus* SCE, which is only slightly discernible for Au(111). They propose that this wave may originate from an "adsorption" of Co species at defects because the pre-wave is not observed in pure electrolyte solution, and it is almost absent for a defect-free Au(111) electrode in the Co^{2+} containing solution. They found that the charge due to this process corresponds to about 1% of a ML only.

In this sense, we think that this process of adsorption corresponds to the Co UPD process which can be promoted by the defects or by the grain boundary localized in our electrodes.[3,47,48]

3.3 Electromicrogravimetric characterization of Co UPD

3.3.1 Electromicrogravimetric response. In Fig. 8 two curves are shown: the *j*–*E* curve (a) has been described above and the curve (b) corresponds to the change of the frequency–potential (Δ*f*–*E*) curve recorded simultaneously with (a). According to this latter curve, during the negative scan from +100 mV to −400 mV, there is no detectable change in frequency and the current detected in the voltammogram corresponds to double-layer charging. However, a smooth variation of slope of frequency change is observed at potentials more negative than −400 mV but more positive than −907 mV. We think that this behavior of the change of frequency in this potential zone is associated with the formation process of a UPD layer of Co on the substrate. It is important to mention that at this potential (−907 mV) the change of frequency is −23.8 Hz (mass increases) and we think that this value is related to the mass of the UPD monolayer. On continuing the negative scan at potentials more negative than −907 mV, a rapid decrease in frequency (change of slope) can be observed associated with the formation of a massive deposit of Co on the UPD monolayer. This process still

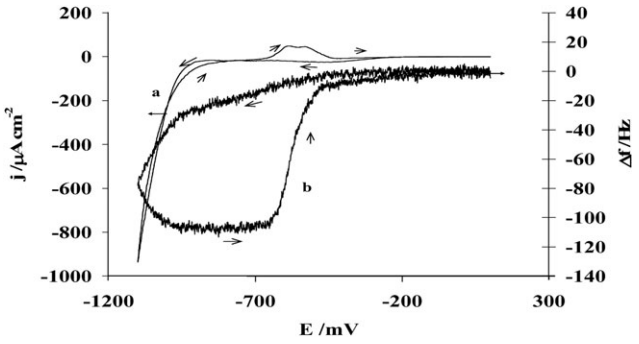

Fig. 8 (a) Current density–potential (j–E) curve for Au EQCM film in $[(NH_4)_2SO_4]$ 1 M pH 9.3 + [Co(II)] 10^{-3} M: scan rate, 5 mV s^{-1}. (b) Change in frequency–potential (Δf–E) curve for Au EQCM film in $[(NH_4)_2SO_4]$ 1 M pH 9.3 + [Co(II)] 10^{-3} M: scan rate, 5 mV s^{-1}. The curve (b) was obtained concomitantly with the j–E curve in (a).

continues when the scan reversal is produced at −1100 mV since the change of frequency keeps decreasing. Following scan reversal the frequency remains constant between −911 mV and −640 mV before increasing (mass decreases) very rapidly in the region *ca.* −640 to −450 mV corresponding to anodic dissolution of the Co deposit. Finally, the destruction of the Co monolayer on the substrate takes place since the frequency increases (mass decreases) slowly at potentials more positive than −450 mV until the original value of Δf is attained in the double-layer region.

Additional curves Δf–E were obtained at different negative potential limits which are shown in Fig. 9.

These curves Δf–E show behavior the same as that described for the curve b in Fig. 8. Furthermore, it is important to mention that the Δf attain a plateau that depends on the cathodic limit potential (see curves a and b) and this plateau is only observed when the cathodic limit potential is more negative than −900 mV (see curve c). We assume that this plateau is associated with the formation of bulk deposition of Co onto the substrate when the limit potential is more negative than the UPD region. So the UPD region is limited by potentials more positive than −900 mV. We obtained the curves of frequency change (Δf) *versus* time (t) at different potential steps in the supposed UPD region which are shown in Fig. 10.

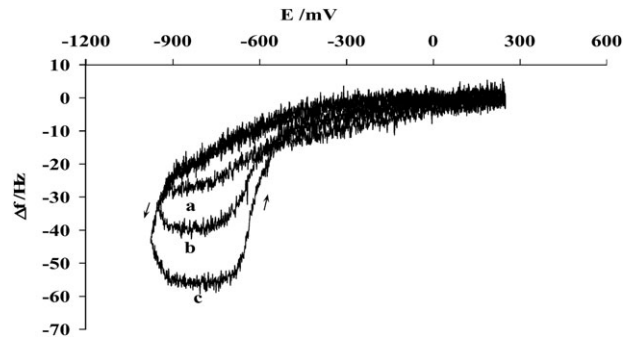

Fig. 9 A set of experimental curves Δf–E obtained simultaneously with I–E curves in the Au/1 mM Co(II) + 1 M $(NH_4)_2SO_4$ (pH 9.3) system at different cathodic limit potentials: (a) −925 mV, (b) −950 mV and (c) −975 mV. The scan potential was 5 mV s^{-1}.

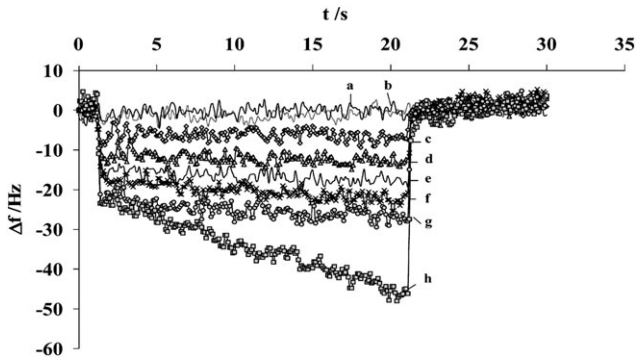

Fig. 10 Some experimental Δf–t curves recorded in the UPD of Co onto Au in 1 mM Co(II) + 1 M $(NH_4)_2SO_4$ (pH 9.3) solution by means of a program of three potential steps. In all cases the starting potential and the final potential were +250 mV. The second potential step was (a) −300 mV, (b) −450 mV, (c) −550 mV, (d) −650 mV, (e) −700 mV, (f) −750 mV, (g) −800 mV, (h) −910 mV.

According to the behavior of the change of frequency, these curves are classified in two categories:

I. The change of frequency (mass) is constant at any time (curves a–e).

II. The change of frequency decreases (mass increases) slowly as a function of time (curves f–h).

For the first category, the value of Δf is almost zero when the step potential is more positive than the potential of peak B (curves a and b), which implies that the mass is not deposited on the substrate. On the contrary, when the step potential is more negative than the potential of the peak B (curves c and d), the value of Δf (mass) is constant at any step time and Δf is only a function of the potential step. This behavior of the Δf implies that the substrate coverage is a function of the energy of the adsorption sites, for example, defect-like sites. It is important to state that these results are opposite to Kleinert's, because if the process of Co deposition occurs *via* a 2D nucleation mechanism then the response of the Δf should slowly diminish as a function of time.

On the other hand, for the second category, the Δf decreases (mass increases) slowly at potential steps more negative than −700 mV but more positive than −800 mV, curves e–g. This behavior, perhaps, is due to the fact that cobalt atoms occupy other adsorption sites, such as reconstruction defects or defects present on terraces.

Finally, the curves g and h present a behavior typical of a growing mass of a metal on an electrode resulting from the gradual decrease of Δf (mass increase) as a function of the step potential due to the bulk deposition occurring at potentials more negative than −800 mV. In this case the process depends on the time of the potential step. It is proper to mention that in this part of the deposit formation process, cobalt may either grow layer by layer, as stated by other authors, or the Co monolayer formed in the UPD zone may give rise to an even more compact structure. However, it is clear that any of these processes develops from a full cobalt monolayer deposited on the substrate, because the Δf changes at an early point of the step potential to a value of approximately −23 Hz, which is in agreement with what was determined by voltammetry.

3.3.2 Charge of Co monolayer. The charge of the Co UPD monolayer can be obtained by EQCM if the number of electrons (z) exchanged in the process is known. This task is accomplished using Faraday's first law

$$\frac{MM}{z} = \frac{\Delta m}{Q} \times F \qquad (2)$$

where MM is the molar mass of Co, z is the number of electrons exchanged, MM/z is the molar mass equivalent, Q is the charge density, Δm is the mass density and F is the Faraday constant.

Some authors[49] utilize an equation equivalent to eqn (2):

$$\frac{MM}{z} = -FC_f \times \frac{f(t_2) - f(t_1)}{|Q(t_2) - Q(t_1)|} \qquad (3)$$

It is important to mention that to obtain z in any case it is necessary to determine MM/z, after which Δm and Q have to be obtained separately. Consequently Q is determined by chronoamperometry and Δm (or Δf) is obtained using EQCM. It is noteworthy that we determine z with the anodic response of the step program since this portion is weakly influenced by the double layer charge and is directly related to the UPD process.

In Fig. 11 we show some curves ΔQ *vs.* Δf (or Δm) used in the determination of z and in Table 1, we summarise some data on z produced using the expression (3).

As can be seen, all values of the number of electrons exchanged, determined (Table 1) at constant potential in the UPD region, approach two. These results indicate that the atoms of Co are adsorbed onto the gold substrate as discharged atoms. These values are in agreement with Schultze,[50] since this author established that if the substrate electronegativity is more important than that of the adsorbate and their difference is less than 0.5, then the adsorbate will be adsorbed as discharged species.

On the other hand, as the potential is more negative than ~ -800 mV the values of z decrease from 2 to around 1.25 and it is possible to say that its values will increase as a function of cathodic potential. This behavior is probably due to the fact that H^+ reduction influences the density of charge (ΔQ) and consequently this calculus, since this reaction is thermodynamically produced at potentials more negative than -780 mV ($E(H^+/H_2)$).

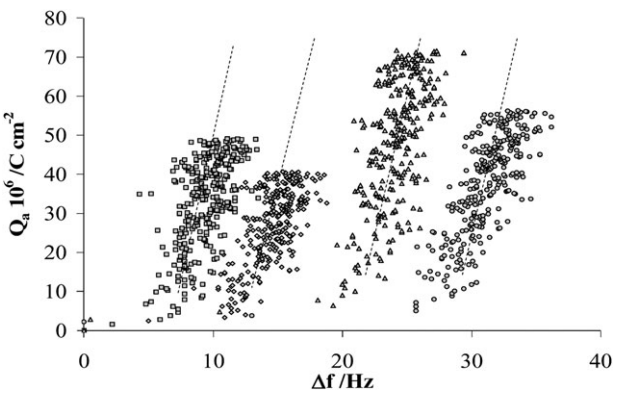

Fig. 11 Some plots of anodic charge density (Q_a) *versus* change of frequency (Δf) at different potential steps (see Table 1).

Table 1 Number of electrons exchanged (z) by the Co with the substrate at different potentials

E/mV	z
−550	1.95
−650	2.24
−750	1.94
−800	2.04
−850	1.15
−900	1.10
−910	1.17
−920	1.21
−930	1.30
−940	1.35

Additionally, the two electrons exchanged by the Co in the process of monolayer formation would be confirmed if the following route is considered:

If the Co atom is considered to be adsorbed as an adatom, which transfers *two electrons* to form a commensurate overlayer onto the highly ordered gold electrode (111), the Δf calculated with the eqn (4), resulting from the expression (1) and Faraday's first law (eqn (2)), is 23.3 Hz. This value of Δf is in agreement with our experimental value of 23.8 Hz or 23.3 Hz (see Figs. 8–10) which shows that the Co atoms exchanged totally their charge.

$$\Delta f = -\left(\frac{C_f MM}{zF}\right) \times \Delta Q \qquad (4)$$

On the other hand, by substituting the data $z = 2$ and $\Delta f = 23.8$ Hz in the expression (4), the experimental density of the Co UPD monolayer charge of 443.39 ± 1.87 μC cm^{-2} is obtained. This charge corresponds effectively to a commensurate Co overlayer on the gold substrate. Our result is supported by the results of Kleinert *et al.*,[23] who indicated that the reconstruction of the substrate was lifted during Co deposition, thereby implying that the cobalt monolayer could copy the substrate structure. In addition, the 1×1 structure is supported by the fact that the same authors mentioned it as a final step in the process of the monolayer formation.

3.3.3 Adsorption isotherm. Fig. 12 shows the isotherm of adsorption and desorption processes of the Co UPD process on a gold substrate. These curves were prepared using the Δf response produced during the scan of the UPD region and the

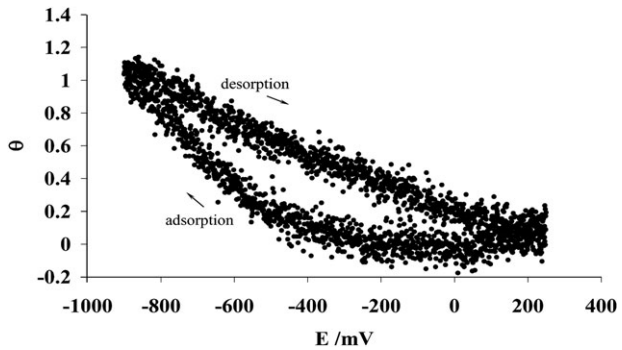

Fig. 12 Isotherm of the Co UPD process on a gold substrate.

expression (4). In addition, the covering degree (θ) was calculated using

$$\theta = \frac{Q_E}{Q_{\mathrm{ml}}} \qquad (5)$$

where Q_{ml} is the density of charge of the monolayer determined by EQCM and Q_E is the density charge at E potential.

From +100 mV to negative potentials, the process of the Co monolayer formation starts progressively at around −400 mV and ends at −875 mV. These values indicate that in a potential region of 400 mV, the monolayer is completed and the behavior of the curve shows that Co atoms adsorb selectively on the sites of the substrate surface (skink, step, terraces, *etc.*). In other words, in the process of monolayer formation on the substrate the first adsorption sites to be occupied by the Co atoms are those of low energy (skink, step) and subsequently, the adsorption sites of high energy (sites like terraces).

The analysis of the desorption process shows that this occurs differently from the adsorption process. The desorption process follows a linear behavior and it is produced slowly with a different slope with regard to the opposite process. It is important to mention that the covering degree at −400 mV is almost 50% of the monolayer in the desorption process and that the remaining 50% is desorbed in a potential region of 600 mV. This behavior indicates that the desorption process and its opposite follow different mechanisms and that the process of monolayer formation is, in essence, irreversible, which is in agreement with the results found in voltammetric experiments. This irreversible characteristic of the isotherms is possibly due to the adsorption competence of H on the substrate produced during the process of adsorption.

4 Conclusions

The Co UPD process on a gold substrate was studied by coupling voltammetry and chronoamperometry with a quartz microbalance in ammonium solution. The results obtained show that the Co forms only one layer at the substrate before the bulk deposition of cobalt occurs. During the UPD process, the Co atom completely transfers its two electrons to the electrode and is adsorbed as discharged species. The Co atoms occupy the sites on the substrate in accordance with their energy. In other words, the low-energy sites are occupied at low covering degrees and the high-energy sites are occupied at high covering degrees. The monolayer charge density, determined by electromicrogravimetry, is 448 μC cm^{-2}, which possibly corresponds to a 1 × 1 structure at the gold substrate. In addition, the UPD formation process is controlled by adsorption as shown by voltammetry. Finally, the analysis of the process of monolayer destruction (desorption) shows that this follows a different mechanism with regard to the formation process possibly due to the adsorption of H onto the substrate produced during the process of adsorption of the metallic monolayer.

Acknowledgements

This research was performed under the auspices of the Universidad Autonoma de San Luis Potosí through the Teaching Support Fund and the Ministry of Public Education through the Program for Teachers' Improvement (PROMEP).

References

1 A. Aramata, in *Modern Aspects of Electrochemistry*, ed. J. O'M. BocKris, R. E. White and B. E. Conway, Plenum Press, New York, 1997, vol. 31, pp. 181–249.
2 D. M. Kolb, in *Advances in Electrochemistry and Electrochemical Engineering*, ed. H. Gerischer and C. W. Tobias, Wiley-Interscience Publication, New York, 1978, vol. 11, pp. 125–271.
3 A. Hamelin, *J. Electroanal. Chem.*, 1979, **101**, 285.
4 S. Takahashi, K. Hasebe and A. Aramata, *Electrochem. Commun.*, 1999, **1**, 301.
5 H. Uchida, M. Hiei and M. Watanabe, *J. Electroanal. Chem.*, 1998, **452**, 97.
6 B. K. Niece and A. A. Gewirth, *J. Phys. Chem. B*, 1998, **102**, 818.
7 A. E. Berkowitz, J. R. Mitchell, M. J. Carey, A. P. Young, S. Zhang, F. E. Spada, F. T. Parker, A. Hutten and G. Thomas, *Phys. Rev. Lett.*, 1992, **68**, 3745.
8 J. Q. Xiao, J. S. Jiang and C. L. Chien, *Phys. Rev. Lett.*, 1992, **68**, 3749.
9 C. L. Chien, J. Q. Xiao and J. S. Jianq, *J. Appl. Phys.*, 1993, **73**, 5309.
10 L. Piraux, J. M. George, J. F. Despres, C. Leroy, E. Ferain, R. Legras, K. Ounadjela and A. Fert, *Appl. Phys. Lett.*, 1994, **65**, 2484.
11 J. Q. Wang, E. Price and G. Xiao, *J. Appl. Phys.*, 1994, **75**, 6903.
12 Y. J. Chen, W. Y. Cheung, I. H. Wilson, N. Ke, S. P. Wong, J. B. Xu, H. Sang and G. Ni, *Appl. Phys. Lett.*, 1998, **72**, 2472.
13 Y. D. Zhang, J. I. Budnick, A. Hines, C. L. Chien and J. Q. Xiao, *Appl. Phys. Lett.*, 1998, **72**, 2053.
14 A. Gerber, A. Milner, I. Y. Korenblit, M. Karpovsky, A. Gladkikh and A. Sulpice, *Phys. Rev. B: Condens. Matter Mater. Phys.*, 1998, **57**, 13667.
15 J. A. De Toro, J. P. Andrés, J. A. González, J. P. Goff, A. J. Barbero and J. M. Riveiro, *Phys. Rev. B: Condens. Matter Mater. Phys.*, 2004, **70**, 224412.
16 S. Kenane and E. Chainet, *Electrochem. Commun.*, 2002, **4**, 167.
17 L. Cagnon, A. Gundel, T. Devolder, A. Morrone, C. Chappert, J. E. Schmidt and P. Allongue, *Appl. Surf. Sci.*, 2000, **164**, 22.
18 L. H. Mendoza-Huizar, J. Robles and M. Palomar-Pardavé, *J. Electroanal. Chem.*, 2002, **521**, 95.
19 L. H. Mendoza-Huizar, J. Robles and M. Palomar-Pardavé, *J. Electroanal. Chem.*, 2003, **545**, 39.
20 L. H. Mendoza-Huizar, J. Robles and M. Palomar-Pardavé, *J. Electrochem. Soc.*, 2005, **152**, C265.
21 I. Flis-Kabulska, *J. Appl. Electrochem.*, 2006, **36**, 131.
22 W. Schindler, D. Hofmann and J. Kirsner, *J. Electrochem. Soc.*, 2001, **148**, C124.
23 M. Kleinert, H.-F. Waibel, G. E. Engelmann, H. Martin and D. M. Kolb, *Electrochim. Acta*, 2001, **46**, 3129.
24 S. Trasatti, *Chim. Ind. (Milan, Italy)*, 1971, **53**, 559.
25 D. A. Buttry and M. D. Ward, *Chem. Rev.*, 1992, **92**, 1355.
26 S. Langerock and L. Heerman, *J. Electrochem. Soc.*, 2004, **151**, C155.
27 G. A. Snook, A. M. Bond and S. Fletcher, *J. Electroanal. Chem.*, 2002, **526**, 1.
28 S. Hadzi-Jordanov, H. Argenstein-Kozlowska, M. Vukovic and B. E. Conway, *J. Electrochem. Soc.*, 1978, **125**, 1471.
29 H. Angerstein-Kozlowska, B. E. Conway, B. Barnett and J. Mozota, *J. Electroanal. Chem.*, 1979, **100**, 417.
30 A. Hamelin, *J. Electroanal. Chem.*, 1996, **407**, 1.
31 S. Štrbac, R. R. Adžić and A. Hamelin, *J. Electroanal. Chem.*, 1988, **249**, 291.
32 M. C. Santos, L. H. Mascaro and S. A. S. Machado, *Electrochim. Acta*, 1998, **43**, 2263.
33 T. Hachiya, H. Honbo and K. Itaya, *J. Electroanal. Chem.*, 1991, **315**, 275.

34 E. Herrero, L. J. Buller and H. D. Abruña, *Chem. Rev*., 2001, **101**, 1897.
35 D. M. Kolb, M. Przasnyski and H. Gerischer, *J. Electroanal. Chem*., 1974, **54**, 25.
36 W. J. Lorenz, H. D. Hermann, N. Wuthrich and F. Hilbert, *J. Electrochem. Soc*., 1974, **121**, 1167.
37 G. L. Borges, K. K. Kanazawa, J. G. Gordon II, K. Ashley and J. Richer, *J. Electroanal. Chem*., 1994, **364**, 281.
38 M. Watanabe, H. Uchida, M. Miura and N. Ikeda, *J. Electroanal. Chem*., 1995, **384**, 191.
39 A. Montes-Rojas and E. Chainet, *J. Mex. Chem. Soc*., 2005, **49**, 341.
40 A. B. Soto, E. M. Arce, M. Palomar-Pardave and I. Gonzalez, *Electrochim. Acta*, 1996, **41**, 2647.
41 S. Fletcher, C. S. Halliday, D. Gates, M. Westcott, T. Lwin and G. Nelson, *J. Electroanal. Chem*., 1983, **159**, 267.
42 B. E. Conway and E. Gileadi, *Trans. Faraday Soc*., 1962, **2493**, 68.
43 S. Srinivasan and E. Gileadi, *Electrochim. Acta*, 1966, **321**, 11.
44 V. A. Vincent and S. Bruckenstein, *Anal. Chem*., 1973, **45**, 2036.
45 E. Kirowa-Eisner, R. Gepshtein and E. Gileadi, *J. Electroanal. Chem*., 2005, **583**, 273.
46 T. Berzins and P. Delahay, *J. Am. Chem. Soc*., 1953, **75**, 555.
47 A. Hamelin, *J. Electroanal. Chem*., 1984, **165**, 167.
48 M. S. Zei, Y. Nakai, G. Lehmpfuhl and D. M. Kolb, *J. Electroanal. Chem*., 1983, **150**, 201.
49 G. G. Lang, M. Ujvari and G. Horanyi, *J. Electroanal. Chem*., 2002, **522**, 179.
50 J. W. Schultze and F. D. Koppitz, *Electrochim. Acta*, 1976, **21**, 327.

